19th Brazilian Congress of Thermal Sciences and Engineering
November 6th–10th, 2022, Bento Gonçalves - RS - Brazil

ENC-2022-0729
OPERATIONAL COST ASSESSMENT OF AIR-SOURCE HEAT PUMPS INTEGRATED TO THERMAL ENERGY STORAGE IN SOUTHERN BRAZIL

Conrado Ermel
Federal University of Rio Grande do Sul - UFRGS, Brazil
conradoermel@gmail.com

Marcus V.A. Bianchi
National Renewable Energy Laboratory - NREL, USA

Paulo S. Schneider
Federal University of Rio Grande do Sul - UFRGS, Brazil

Abstract. *Air source heat pump (ASHP) deployment is expected to grow in the next years as a response to the decarbonization needs in the building sector. While not extremely cold, the southern region of Brazil has relevant heating demands during winter; therefore, we present a techno-economic analysis on HP-based systems operating for three different locations in the region. A dynamic simulation model was implemented to represent the ASHP and the integration with a thermal energy storage (TES). The system's performance was compared to combustion appliances and electric resistance heaters operating over a year. Results show that in the Brazilian context, traditional combustion appliances present* $13\,\%$ *to* $41\,\%$ *higher operation costs and* $69.5\,\%$ *more* CO_2 *emission, compared to electric resistance heaters. Furthermore, replacing electric resistances by ASHP could reduce the energy consumption up to* $74\,\%$*, with the costs and* CO_2 *emissions following the same trend. When TES was integrated to the ASHP, the energy consumption increased from* $7\,\%$ *to* $23\,\%$*, depending on the location. Results suggest the use of TES could be advantageous if a better operation logic is implemented and time-of-use rates are considered.*

Keywords: *Heat pump, Thermal energy storage, Decarbonization, Buildings, Space heating*

1. INTRODUCTION

Buildings are relevant energy consumers and responsible for fair amounts of the carbon dioxide emission worldwide. According to Carroll *et al.* (2020), they account for around $40\,\%$ of end-use CO_2 emissions in the US and $36\,\%$ in the EU (Le *et al.*, 2019). Almost half of the energy demand is due to thermal loads (Kishore *et al.*, 2020), and the most common heating systems are the natural gas furnaces, electric resistance heaters, and electric heat pumps (HP). If supplied by electricity generated through renewables, HP are less pollutant than furnaces, being up to five times more efficient than electric resistances Dincer *et al.* (2017). Several countries are making a move towards replacing combustion appliances by HPs, aiming at decarbonization. In fact, it is expected that the deployment of heat pumps will significantly increase in the next years in the US (DOE, 2021), Europe (IEA, 2022), and China (Wang *et al.*, 2020).

Because of the increasing number of HP, electricity transmission system will face energy demand challenges, specially in peak-periods (Bianco *et al.*, 2017). If the energy mix has a high penetration of renewables, which is necessary for decarbonization, the grid also has to deal with intermittence. Moreover, in very cold temperatures the performance of HPs deteriorates, requiring assistance of peripheral equipment that usually requires more energy to operate. Thermal energy storage (TES) has been studied as auxiliary systems to support HP, and addresses some of the mentioned issues (Ermel *et al.*, 2022a).

As a tropical country, Brazil requires more cooling than heating. Nonetheless, there are regions in southern Brazil which require heating systems during winter. Usually, residential buildings in southern Brazilian adopt electric resistance heaters and combustion appliances to supply the heating loads. Moreover, houses in Brazil hardly employ good thermal insulation, which increases the heating demand even under mild temperatures. Brazil has an electric energy mix mainly composed by renewable sources: $65\,\%$ hydro-power, $9.1\,\%$ biomass, $8.8\,\%$ wind, and $1.7\,\%$ solar (EPE, 2022). Hence, replacing combustion appliances by HP would directly reduce the total carbon emitted by buildings in the country.

Very few works have explored the role of heat pumps in the Brazilian climate. There are studies on their usage for domestic water heating systems (Duarte *et al.*, 2021), however their use for space heating has been overlooked, and is usually seen as a complementary part of cooling systems. In this paper we employed a Python framework (Ermel *et al.*, 2022b) to simulate the operation of four different space heating systems: a) electric-resistance based heater, b) a furnace using liquefied petroleum gas (LPG, a mixture of propane and butane), c) air-water heat pump d) air-water heat pump integrated with thermal storage. Annual climate data from Caxias do Sul-RS, Urubici-SC, and Curitiba-PR (Hersbach *et al.*, 2018) were used to feed the model and compare the performance of the four systems regarding the operation cost and CO_2 emission.

2. METHODOLOGY

2.1 Air source heat pump model

Heat pumps employ a vapor compression cycle to transfer energy from an environment that is generally cooler (outside) to an environment that is warmer (inside). The fundamental cycle, displayed in Fig 1, consists of a compressor, a condenser, an expansion device, and an evaporator, notwithstanding the presence of various peripheral components in the equipment. The model adopted in this paper is a quasi-steady-state representation of the vapor compression cycle, which was proposed by the authors (Ermel *et al.*, 2022b). Each component (compressor, condenser, evaporator, and expansion valve) is an object that join into a larger object to depict the operation of a heat pump, allowing for the user to change the construction and operation parameters.

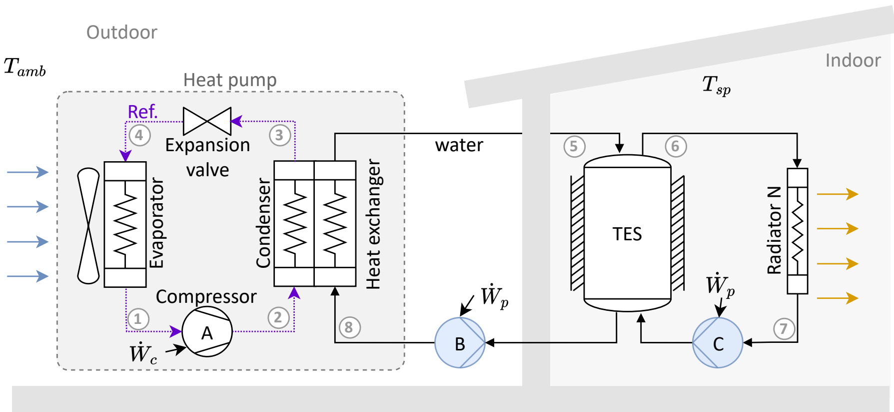

Figure 1: System diagram

The enthalpy marching solution procedure (Winkler *et al.*, 2008) is adopt with all the components being solved at each iteration. The pressure levels at points 1 and 2 are guessed, and the refrigerant mass flow rate is calculated by

$$\dot{m}_r = \rho_1 V_{comp} \left(n/60\right) \eta_{vol}, \tag{1}$$

where V_{comp} is the displacement [m^3], n the compressor rotation speed [rpm], η_{vol} the volumetric efficiency. Equation 2 is the energy balance applied to the evaporator (external unit)

$$\dot{Q}_e = \dot{m}_r(h_1 - h_4) \quad = \quad \dot{m}_r U_e A_e (T_{m_e} - T_{air_{outdoor}}). \tag{2}$$

To account for the different regions of the refrigerant along the heat exchanger, we employ the Kriging-assisted three-zone model proposed by Huang *et al.* (2020). The overall heat transfer coefficient U_{zone} for each zone is given by (Li *et al.*, 2020)

$$U_{zone} = \left(\frac{1}{h_z} + \frac{1}{h_{air}\eta_{fin}R_{fin}}\right)^{-1}, \tag{3}$$

where h_z and h_{air} are the refrigerant-side and air-side heat transfer coefficients, respectively. η_{fin} is the fin's efficiency, and R_{fin} the fin ratio. We assume a representative heat transfer coefficient of $h_{vap} = h_{liq} = 600\,\mathrm{W\,m^{-2}\,K^{-1}}$ for the vapor and liquid phases and $h_{2ph} = 3000\,\mathrm{W\,m^{-2}\,K^{-1}}$ for the two-phase zone. On the air side, h_{air} equals $100\,\mathrm{W\,m^{-2}\,K^{-1}}$. Although they can change based on the fluids and the flow circumstances, these values are representative for the studied case. The zone length is calculated by Eq. (4), the outlet enthalpy by Eq. (5), and the outlet temperature Eq. (6) (Huang *et al.*, 2020).

$$L_{zone} = \frac{\dot{m}_r dh}{dT U_{zone} \pi D}, \tag{4}$$

$$h_{zone} = h_{in} - U_{zone}A_{zone}\frac{dT}{\dot{m}_r}, \tag{5}$$

$$T_{zone} = \frac{U_{zone}A_{zone}(T_{air_{in}} - 0.5T_{in}) + \dot{m}_r * C_{p_r} * T_{in}}{(\dot{m}_r C_{p_r} + 0.5U_{zone}A_{zone})}. \tag{6}$$

C_{p_r} is the refrigerant specific heat, D and A_{zone} are the tube inner diameter and the zone surface area, respectively. h_i represents the refrigerant enthalpy entering the zone, $T_{air_{in}}$ is the ambient air temperature and T_{in} is the refrigerant temperature in the zone, assumed to be uniform. Solution is reached when calculations meet the convergence criteria (residual < 1×10^{-6}).

2.2 Thermal load model

The heating load is calculated using the residential load factor method from standard 169-2021 (ANSI/ASHRAE, 2021) (Eq. 7) while taking into account the detached single-family home of Fig. 2 measuring $120\,\mathrm{m}^2$ and having the following features: U_w = ($0.51\,\mathrm{W\,m^{-2}\,K^{-1}}$) for the walls and ($A_r$ = $120\,\mathrm{m}^2$ and U_r = $0.18\,\mathrm{W\,m^{-2}\,K^{-1}}$) for the roof. The indoor temperature setpoint T_{sp} was arbitrarily chosen constant at $19\,°\mathrm{C}$.

$$\dot{Q}_{load} = A_w U_w\left(T_{amb} - T_{sp}\right) + A_r U_r\left(T_{amb} - T_{sp}\right) \tag{7}$$

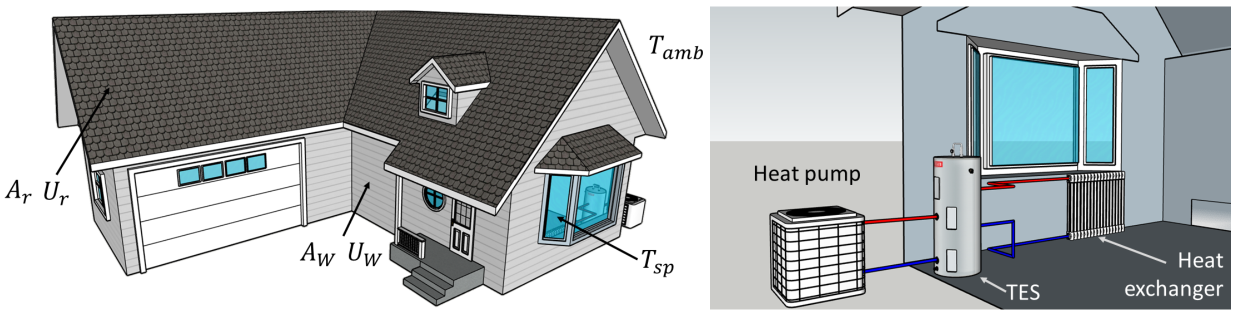

(a) (b)

Figure 2: a) Single-family detached dwelling b) view of the simulated ASHP-TES heating system

Figure 3 shows the thermal loads simulated for the single-family detached dwelling previously described. In general, in South America the heating loads are much lower than the ones of North America, Europe, and North Asia, although, Chile and part of Argentina present relevant heating demands. Brazil, as a tropical country, has much higher demands for cooling than for heating. Nonetheless, the southern states of Rio Grande do Sul (RS), Santa Catarina (SC), and Parana (PR) present significant heating demands during winter.

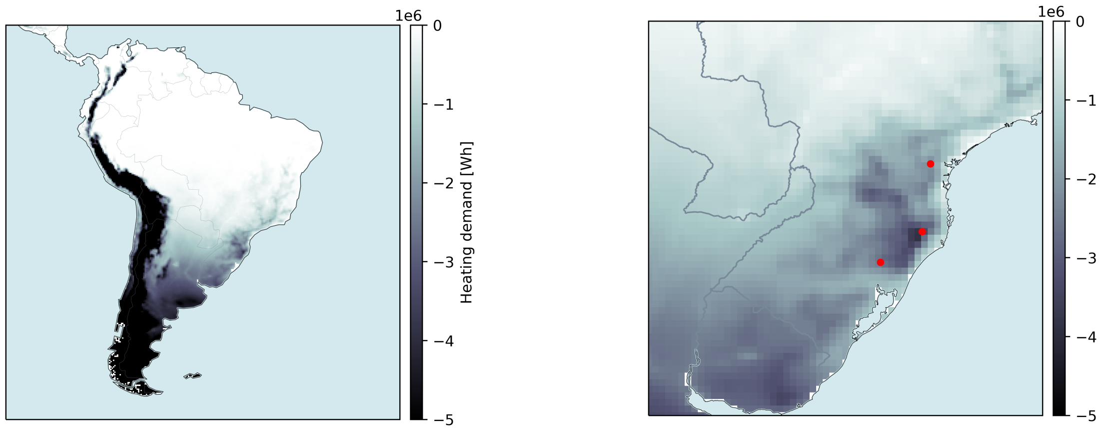

(a) (b)

Figure 3: Annual heating load for a $120\,\mathrm{m}^2$ single-family detached dwelling

2.3 Case study

Given the heating load map of Fig. 3 we choose three cities located in cold regions to perform the techno-economic analysis: Caxias do Sul (RS), Urubici (SC), and Curitiba (PR). We compare the operational costs and estimated CO_2 emission of the heating systems presented in Fig. 4. All the heat introduced by the systems is considered to be perfectly distributed in the house, and the electric resistance is assumed to have unitary COP, while the furnace has an efficiency of 90 % (Yu *et al.*, 2021). Both the ASHP and the ASHP-TES systems are air-water heat pumps, which require an hydraulic

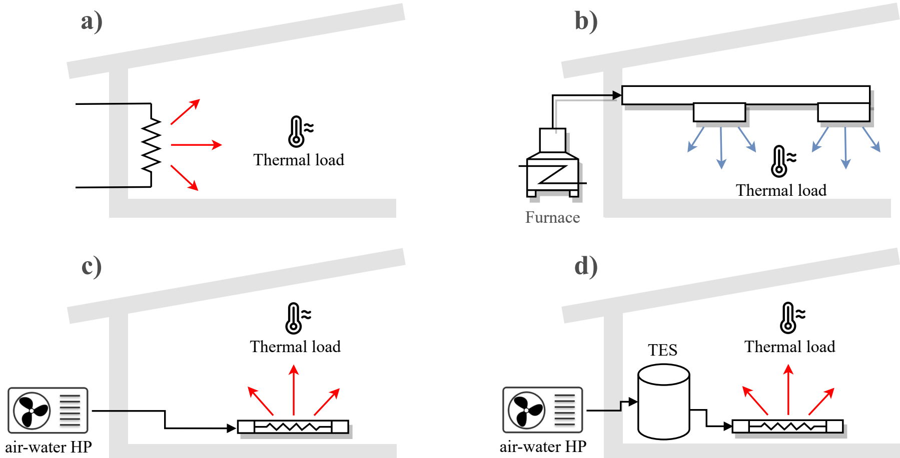

Figure 4: Heating systems compared in this study a) Electric resistance heater b) LPG gas furnace c) Air-water heat pump d) Air-water heat pump integrated with thermal storage

system to distribute the heat in the house.

Table 1 presents the parameters used to simulate the ASHP and the ASHP-TES systems. The heat pump model inputs are: compressor rotation n, displacement $Disp$, isentropic efficiency η_{iso}, and volumetric efficiency η_{vol}. A refrigerant-

Table 1: Parameters of the ASHP and ASHP-TES systems.

Device	Parameter	Value
Compressor	n	3600
	$Disp$	2.5×10^{-5}
	η_{iso}	0.63
	η_{vol}	0.95
Condenser	Effectiveness	0.7
Water tank	Area	$6.28\,\mathrm{m^2}$
	Volume	$1.17\,\mathrm{m^3}$
	Overall heat transfer coeff. U	$0.5\,\mathrm{W\,m^{-2}\,K^{-1}}$
Pump B	Mass flow rate	$0.1\,\mathrm{kg\,s^{-1}}$

water heat exchanger is used, therefore, a constant effectiveness of 0.9 is adopted. A $1.17\,\mathrm{m^3}$ water tank is adopted as sensible TES, and the heat losses are calculated with an overall heat transfer coefficient of $0.5\,\mathrm{W\,m^{-2}\,K^{-1}}$.

For the electric equipment, the operation cost is calculated as

$$C_{op} = \sum_{t=0}^{8760} \dot{W}_c(t) El_r, \tag{8}$$

where $\dot{W}_c$ is the energy consumed by the compressor [kW h], and El_r is the electricity rate [R$/kWh]. For the LPG furnace, the operation cost is

$$C_{op-NG} = \sum_{t=0}^{8760} \frac{Q_{load}}{LHV} \frac{NG_r}{\eta_f}, \tag{9}$$

with Q_{load} the heating load [kW h], LHV the lower heating value ($46 \times 10^6\,\mathrm{MJ\,kg^{-1}}$), NG_r the LPG price [R$/kg], and η_f the furnace conversion efficiency. The equivalent CO_2 emission is calculated by Eq. (10) for the electric devices.

$$CO2_{eq} = \sum_{t=0}^{8760} \dot{W}_c(t) f_{CO_2}. \tag{10}$$

f_{CO_2} stands for the equivalent CO_2 emission [$kgCO_2/kWh$] of the local energy mix. The furnace emissions are calculate by

$$CO2_{eq-NG} = \sum_{t=0}^{8760} Q_{load} f_{CO_2 NG}. \tag{11}$$

The values adopted for the parameters are presented in Tab. 2.

Table 2: Conversion factors for costs and CO_2 emission

Parameter	Description	value	Reference
El_r	Electricity rate - RS	0.670 R$/kWh	(ANEEL, 2022)
	Electricity rate - SC	0.535 R$/kWh	
	Electricity rate - PR	0.571 R$/kWh	
NG_r	Gas rate	8.72 R$/kg	(Agência Nacional do Petróleo, 2022)
f_{CO_2}	CO_2 emission factor	0.118 $kgCO_2/kWh$	(EPE, 2022)
$f_{CO_2 NG}$	CO_2 emission factor for NG	0.2 $kgCO_2/kWh$	(Yu *et al.*, 2021)

2.4 Control Logic of the ASHP-TES system

For the thermal storage system, the operation logic of Fig. 5 defines when the HP is operating and when to charge or discharge the thermal storage device. The control strategy highly affects the system performance and in the present paper

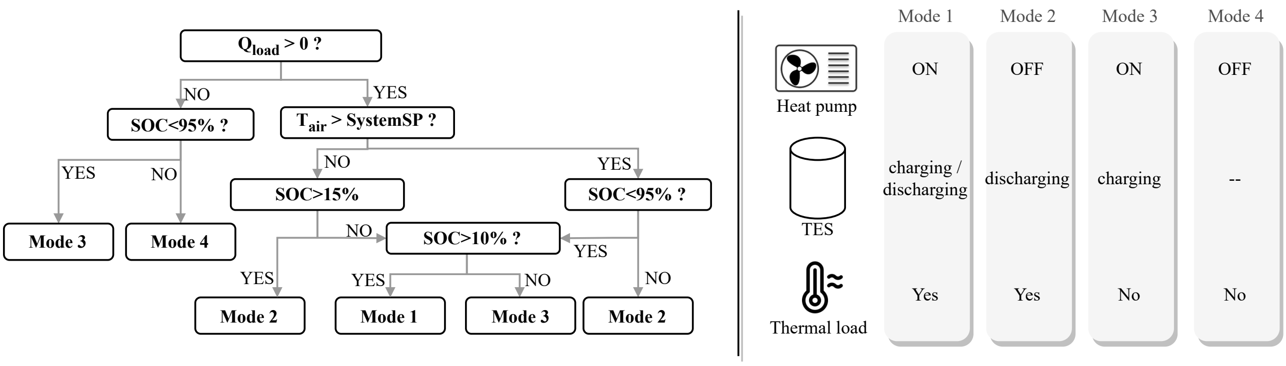

Figure 5: Operation logic

we adopted a basic strategy that aims to prevent the operation of the HP whenever the outdoor temperature is below 10 °C. In this conditions the COP is also lower.

3. RESULTS

Figure 6a shows that the heating demand for the three locations are similar. According to the assumptions, a single-family detached dwelling in Curitiba has an annual heating demand of over 1.5 MW h. Caxias do Sul and Urubici have even higher demands. Because electric resistance heaters have COP=1, the results for the annual energy consumed is assumed to be equal to the heating demand. Figure 6b shows that replacing electric resistances with an ASHP would reduce the annual electricity consumption in almost 74 % for the three cities. The energy savings are similar in all locations because they have a similar temperature profile along the year, hence, the heat pump average COP is similar.

The operational cost of each system is presented in Fig. 7a for all locations. As stated in Eq. (8-11), operational cost and CO_2 emission hold a proportional relationship with the energy consumption. Therefore, the electric resistance heater has higher operational costs and CO_2 emission when compared to the ASHP and the ASHP-TES.

The LPG furnace has the highest operational cost among all the systems, being 13 % higher than the electric resistance in Caxias do Sul, and reaching 41 % in Urubici, where the cost of electricity is lower. This is driven by the high costs of natural gas in Brazil. The difference between the furnace and the other systems is also expressive for the carbon dioxide emissions. Fig. 7b shows that the furnace emits 69.5 % more CO_2 than the resistance heater, and up to 6.5 times more than the ASHP.

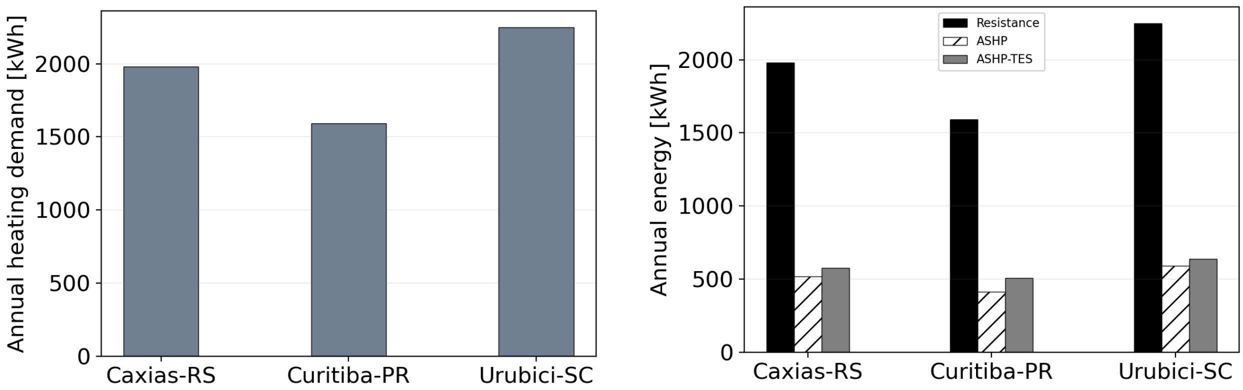

(a) (b)

Figure 6: Annual results of a) heating demands b) electricity consumed by the heating systems

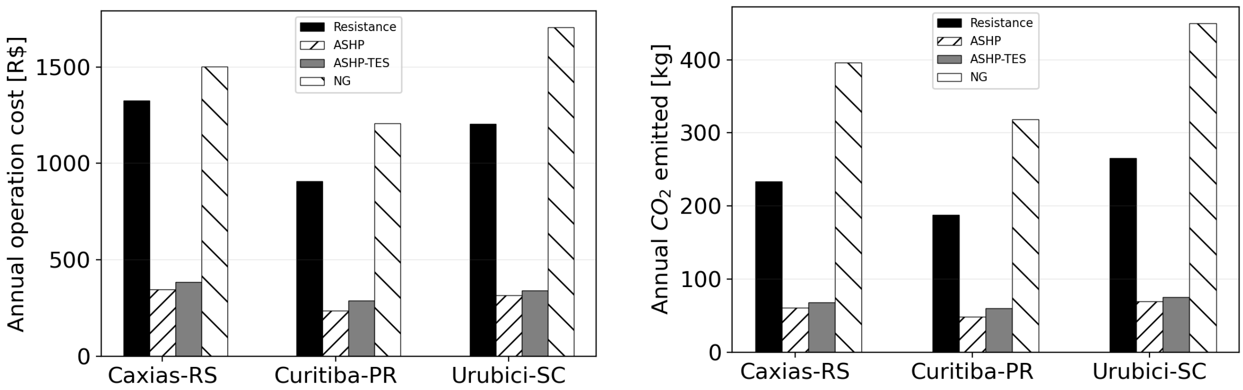

(a) (b)

Figure 7: Annual results of operation cost and CO_2 emission for each location per system

3.1 ASHP-TES system

The ASHP-TES system performed differently according to the location. However, it consumed more energy than the ASHP in all locations: $11\,\%$, $23\,\%$, and $7\,\%$ for Caxias do Sul, Curitiba, and Urubici, respectively. The heating season comprehends the months from May to August, Fig. 8, and the system was configured so the TES is discharged whenever the outdoor temperature is lower than SP_{system} = $10\,°\mathrm{C}$. In all the other times the systems seek to keep the state of charge (SOC) above $95\,\%$, which, in this case, means a water temperature of $49.5\,°\mathrm{C}$. While the ASHP works with a constant water temperature of $44\,°\mathrm{C}$, the ASHP-TES has the water temperature T_8 = $50\,°\mathrm{C}$ in most of the operation time. Since the COP is inversely proportional to the difference between the outdoor and indoor temperatures, in this arrangement it varied from 2.25 to 3.5 depending on the ambient temperature. For the ASHP-TES, the control logic favors the HP operation when the COP is higher, hence, there are times in which the ASHP COP is higher, and in other times its lower than the ASHP-TES. As explored by Ermel *et al.* (2022c), this control strategy presented better results for colder climates, as the difference on energy consumption was around $1.9\,\%$ with the system simulated for the climate of Denver-CO.

No discussion regarding capital investments was addressed in this paper, as only the operational cost, energy consumption, and CO_2 emission were included. However, the studied systems have different concepts, hence, they face different challenges. The furnace, for instance, does not require a hydraulic circuit to distribute the heat throughout the dwelling like the ASHP-TES does. However, it causes the indoor air to displace, which can affect the thermal comfort. Moreover, ducts are required to deliver the heated air to all the rooms. The benefits and drawbacks of the technologies must be discussed altogether to decide on each to employ.

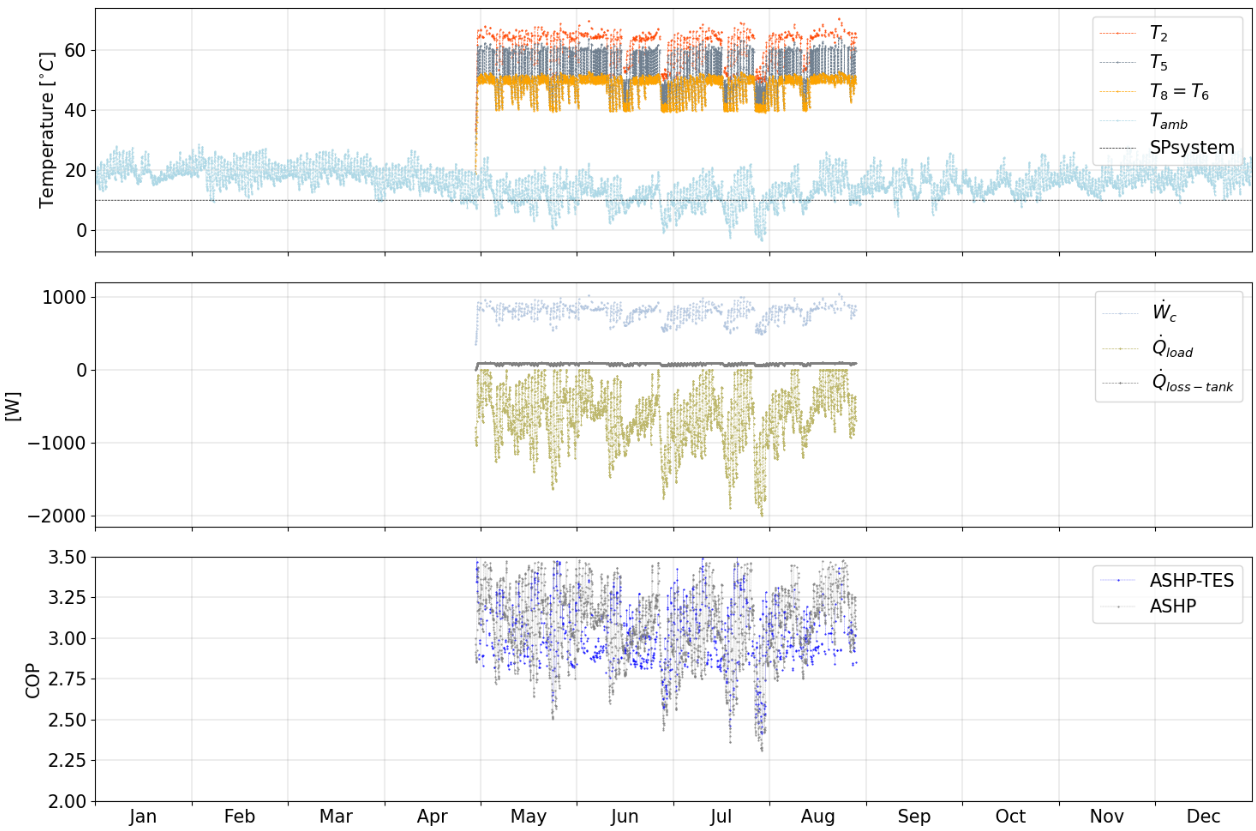

Figure 8: Performance results and variables in the ASHP-TES system

4. CONCLUSIONS

Brazil is a tropical country with the predominance of cooling demands. Nonetheless, there are regions in the south that present relevant heating demands during winter. The performance of four different heating systems (electric resistance, LPG-furnace, ASHP, and ASHP-TES) was simulated for three cities located in south Brazil: Caxias do Sul-RS, Urubici-SC, and Curitiba-PR. Results show that an ASHP could supply the heating load consuming up to 74 % less energy than an electric resistance heater. Moreover, savings on the operation cost about 68 % to 72 % were found when the local average electricity rates were assumed. The LPG furnace presents the highest operation cost and CO_2 emission. In comparison with the ASHP, the LPG-furnace has 13 % to 41 % higher operation cost and is 69.5 % more pollutant. In several countries natural gas is cheaper than electricity, which increases the attractiveness of LPG-furnaces. However, for the Brazilian reality, using LPG for heating systems would be more expensive then using electric resistance, or ideally, heat pumps.

Simulations on the integrated ASHP-TES system revealed that for the studied scenarios, introducing a TES device to the HP would increase the energy consumption in 7 % to 23 %, depending on the location. Operational cost and CO_2 emission follow the same trend. It's important to highlight that the system simulated in the present paper is intended to operate in a much colder climate, which may not match the same requirements of a mild climates. The TES has the potential to support HP operation even in these climates. However, different objectives must be set, for instance, considering time-of-use electricity rates, so the TES is used to shift the load and prevent the HP of operating during peak-hours.

In the present work we only addressed operational costs to assess the performance of HP-based systems in the climate of south Brazil. However, initial costs for ASHP and ASHP-TES are expected to be much higher than electric resistances. Therefore, further analysis are require to quantify the payback time of such solutions, and to help determine the best deployment strategies. Utilities providers, for instance, can take advantage on the flexibility introduced by TES in residential heating systems. This may help reduce the electricity demand in critical periods. On the other hand, governments could support the deployment of ASHP-TES as an action to mitigate the climate crises. Hence, a value proposition must be found in order to highlight the technology benefits and to split the initial investments, making ASHP-TES an attractive alternative. From the author's point of view, for climate regions like the ones in south Brazil, ASHP-TES could find a niche in hybrid space-water heating systems. Moreover, further exploration on the control strategies are required to improve the energy savings.

5. ACKNOWLEDGEMENTS

This study was financed in part by the Coordenação de Aperfeicmento de Pessoal de Nivel Superior-Brasil (CAPES) - Finance Code 001. Conrado Ermel acknowledges Conselho Nacional de Desenvolvimento Científico e Tecnologico (CNPq), Brazil for his Ph.D. grant. Paulo S. Schneider acknowledges CNPq for his research grant (PQ301619/2019-0). This work was authored in part by the National Renewable Energy Laboratory, operated by Alliance for Sustainable Energy, LLC, for the U.S. Department of Energy (DOE) under Contract No. DE-AC36- 08GO28308. Funding provided by the U.S. Department of Energy Office of Energy Efficiency and Renewable Energy Building Technologies Office. The views expressed in the article do not necessarily represent the views of the DOE or the U.S. Government. The U.S. Government retains and the publisher, by accepting the article for publication, acknowledges that the U.S. Government retains a nonexclusive, paid-up, irrevocable, worldwide license to publish or reproduce the published form of this work, or allow others to do so, for U.S. Government purposes.

6. REFERENCES

Agência Nacional do Petróleo, A., 2022. "Síntese dos Preços Praticados - Brasil".

ANEEL, 2022. "Ranking da tarifa elétrica residencial".

ANSI/ASHRAE, 2021. "ANSI/ASHRAE Standard 169-2021 - Climatic Data for Building Design Standards". Technical report, ANSI/ASHRAE, Peachtree Corners. doi:1041-2336.

Bianco, V., Scarpa, F. and Tagliafico, L.A., 2017. "Estimation of primary energy savings by using heat pumps for heating purposes in the residential sector". *Applied Thermal Engineering*, Vol. 114, pp. 938–947. ISSN 13594311. doi: 10.1016/j.applthermaleng.2016.12.058. URL `http://dx.doi.org/10.1016/j.applthermaleng.2016.12.058`.

Carroll, P., Chesser, M. and Lyons, P., 2020. "Air Source Heat Pumps field studies: A systematic literature review". *Renewable and Sustainable Energy Reviews*, Vol. 134. ISSN 1364-0321. doi:10.1016/j.rser.2020.110275.

Dincer, I., Rosen, M.A. and Ahmadi, P., 2017. *Optimization of Energy Systems*. John Wiley and Sons Ltd, 1st edition.

DOE, 2021. "A National Roadmap for Grid-Interactive Efficient Buildings". Technical report, Office of Energy Efficiency and Renewable Energy.

Duarte, W.M., Paulino, T.F., Tavares, S.G. and Maia, A.A.T., 2021. "Feasibility of solar-geothermal hybrid source heat pump for producing domestic hot water in hot climates Faisabilité d ' une pompe à chaleur solaire-géothermique hybride pour la production d ' eau chaude sanitaire dans les climats chauds". *International Journal of Refrigeration*, Vol. 124, pp. 184–196. ISSN 0140-7007. doi:10.1016/j.ijrefrig.2020.12.022. URL `https://doi.org/10.1016/j.ijrefrig.2020.12.022`.

EPE, 2022. "BEN_Síntese_2022_PT". Technical report, EPE - Empresa pública de Energia, Rio de Janeiro.

Ermel, C., Bianchi, M.V., Cardoso, A.P. and Schneider, P.S., 2022a. "Thermal storage integrated into air-source heat pumps to leverage building electrification: A systematic literature review". *Applied Thermal Engineering*, Vol. 215, p. 118975. ISSN 13594311. doi:10.1016/j.applthermaleng.2022.118975. URL `https://linkinghub.elsevier.com/retrieve/pii/S1359431122009103`.

Ermel, C., Bianchi, M.V. and Schneider, P.S., 2022b. "Energy Model of an Air Source Heat Pump to Explore Performance Improvements under Cold Conditions: a Python^{TM} Framework". In *7th International High Performance Buildings Conference at Purdue*. Indiana.

Ermel, C., Bianchi, M.V. and Schneider, P.S., 2022c. "Energy Model to Evaluate Thermal Energy Storage Integrated with Air Source Heat Pumps". In *2022 Buildings XV International Conference - ASHRAE*. Clearwater, FL.

Hersbach, H., Bell, B., Berrisford, P., Biavati, G., Horányi, A., Muñoz Sabater, J., Nicolas, J. and Peubey, C., 2018. "ERA5 hourly data on pressure levels from 1979 to present." doi:10.24381/cds.bd0915c6. URL `https://cds.climate.copernicus.eu/cdsapp#!/dataset/10.24381/cds.bd0915c6?tab=overview`.

Huang, R., Ling, J. and Aute, V., 2020. "Comparison of approximation-assisted heat exchanger models for steady-state simulation of vapor compression system". *Applied Thermal Engineering*, Vol. 166, No. November 2019, p. 114691. ISSN 13594311. doi:10.1016/j.applthermaleng.2019.114691. URL `https://doi.org/10.1016/j.applthermaleng.2019.114691`.

IEA, I.E.A., 2022. "A 10-Point Plan to Reduce the European Union' s Reliance on Russian Natural Gas". Technical Report March, International Energy Agency Website:.

Kishore, R.A., Bianchi, M.V., Booten, C., Vidal, J. and Jackson, R., 2020. "Optimizing PCM-integrated walls for potential energy savings in U.S. Buildings". *Energy and Buildings*, Vol. 226, p. 110355. ISSN 03787788. doi: 10.1016/j.enbuild.2020.110355.

Le, K.X., Huang, M.J., Shah, N.N., Wilson, C., Artain, P.M., Byrne, R. and Hewitt, N.J., 2019. "Techno-economic assessment of cascade air-to-water heat pump retrofitted into residential buildings using experimentally validated simulations". *Applied Energy*, Vol. 250, No. January, pp. 633–652. ISSN 03062619. doi:10.1016/j.apenergy.2019.05.041. URL `https://doi.org/10.1016/j.apenergy.2019.05.041`.

Li, Y., Zhang, N. and Ding, Z., 2020. "Investigation on the energy performance of using air-source heat pump to charge

PCM storage tank". *Journal of Energy Storage*, Vol. 28. ISSN 2352152X. doi:10.1016/j.est.2020.101270.

Wang, Z., Wang, F., Li, G., Song, M., Ma, Z., Ren, H. and Li, K., 2020. "Experimental investigation on thermal characteristics of transcritical CO2 heat pump unit combined with thermal energy storage for residential heating". *Applied Thermal Engineering*, Vol. 165. ISSN 13594311. doi:10.1016/j.applthermaleng.2019.114505.

Winkler, J., Aute, V. and Radermacher, R., 2008. "Comprehensive investigation of numerical methods in simulating a steady-state vapor compression system". *International Journal of Refrigeration*, Vol. 31, No. 5, pp. 930–942. ISSN 01407007. doi:10.1016/j.ijrefrig.2007.08.008.

Yu, M., Li, S., Zhang, X. and Zhao, Y., 2021. "Techno-economic analysis of air source heat pump combined with latent thermal energy storage applied for space heating in China". *Applied Thermal Engineering*, Vol. 185. ISSN 13594311. doi:10.1016/j.applthermaleng.2020.116434.

7. RESPONSIBILITY NOTICE

The author(s) is (are) solely responsible for the printed material included in this paper.